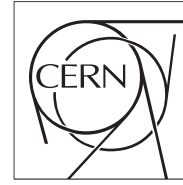




The Compact Muon Solenoid Experiment
Conference Report

Mailing address: CMS CERN, CH-1211 GENEVA 23, Switzerland



19 January 2018 (v2, 26 January 2018)

The CMS Outer Tracker for HL-LHC

Alexander Dierlamm for the CMS Collaboration

Abstract

The LHC is planning an upgrade program, which will bring the luminosity to about $5-7 \times 10^{34} \text{ cm}^{-2} \text{ s}^{-1}$ in 2026, with a goal of an integrated luminosity of 3000 fb^{-1} by the end of 2037. This High Luminosity LHC scenario, HL-LHC, will require a preparation program of the LHC detectors known as Phase-2 Upgrade. The current CMS Tracker is already running beyond design specifications and will not be able to cope with the HL-LHC radiation conditions. CMS will need a completely new Tracker in order to fully exploit the highly demanding operating conditions and the delivered luminosity. The new Outer Tracker system is designed to provide robust tracking as well as Level-1 trigger capabilities using closely spaced modules composed of silicon macro-pixel and/or strip sensors. Research and development activities are ongoing to explore options and develop module components and designs for the HL-LHC environment. The design choices for the CMS Outer Tracker Upgrade are discussed along with some highlights of the R&D activities.

Presented at *HSTD11 11th International Hiroshima Symposium on the Development and Application of Semiconductor Tracking Detectors*

The CMS Outer Tracker Upgrade for the HL-LHC

Alexander Dierlamm on behalf of the CMS Tracker Collaboration^{a,*}

^a*Institut für Experimentelle Teilchenphysik, Karlsruher Institut für Technologie, Hermann-von-Helmholtz-Platz 1, 76344 Egg.-Leopoldshafen*

Abstract

The LHC is planning an upgrade program, which will bring the luminosity to about $5 - 7 \times 10^{34} \text{ cm}^{-2} \text{ s}^{-1}$ in 2026, with a goal of an integrated luminosity of 3000 fb^{-1} by the end of 2037. This High Luminosity LHC scenario, HL-LHC, will require a preparation program of the LHC detectors known as Phase-2 Upgrade. The current CMS Tracker is already running beyond design specifications and will not be able to cope with the HL-LHC radiation conditions. CMS will need a completely new Tracker in order to fully exploit the highly demanding operating conditions and the delivered luminosity. The new Outer Tracker system is designed to provide robust tracking as well as Level-1 trigger capabilities using closely spaced modules composed of silicon macro-pixel and/or strip sensors. Research and development activities are ongoing to explore options and develop module components and designs for the HL-LHC environment. The design choices for the CMS Outer Tracker Upgrade are discussed along with some highlights of the R&D activities.

Keywords: silicon sensors, tracking, radiation hardness

1. Introduction to HL-LHC and the Outer Tracker Upgrade of CMS

The Large Hadron Collider (LHC) at CERN will undergo an extensive upgrade program during the long shutdown 3 (2024-2026) to reach unprecedented performance. The instantaneous luminosity will reach $5 - 7 \times 10^{34} \text{ cm}^{-2} \text{ s}^{-1}$ and the integrated luminosity will reach 3000 fb^{-1} [1, 2] (up to 4000 fb^{-1} , if the ultimate instantaneous luminosity can be achieved). As consequences of the increased performance the detector has to cope with increased radiation levels and more collisions within one bunch crossing (pile-up). The current trigger system of CMS [3] would not be capable of efficiently selecting the interesting events. It was shown that the track information from the tracking system can significantly improve the performance of the Level-1 (L1) trigger [4], which is the first instance of the trigger system. That necessitates to provide the relevant tracks for each bunch crossing. This is the main requirement that drives the layout and concepts of the new Outer Tracker for the HL-LHC phase. Further requirements and corresponding implementations are listed in Tab. 1.

2. Design of the new Outer Tracker for CMS

Figure 1 shows the layout of the planned CMS Tracker. The Outer Tracker (radius r larger than 200 mm) contains only two types of modules, which are made of a stack of

Table 1: Requirements for the new CMS Tracker and their implementations followed by buzzwords being explained in this article.

Requirement	Implementation	Buzzwords
Alive up to 3000 fb^{-1}	Rad. resistance; cold (-20°C) operation	n-in-p type silicon; CO ₂ cooling
O(1%) occupancy up to PU 140 (possibly more); robust pattern recognition	Increased granularity; optimized layout	Macro-pixel sensors
Contribute to L1 trigger	Track trigger capabilities	p _T -modules
Upgraded L1 trigger: higher rate (750 kHz), longer latency (12.5 μs)	Large readout bandwidth; deep front-end buffers	Binary readout; gigabit links
Reduce material effects	Optimization of passive volumes and services	CO ₂ cooling; tilted barrel; DC-DC-powering

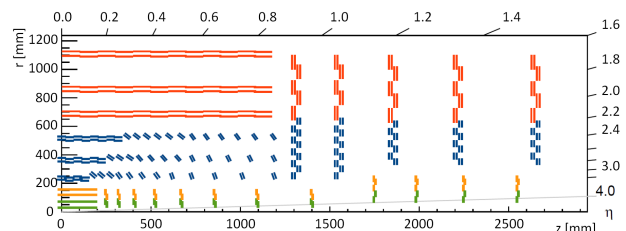


Figure 1: Layout of the new CMS Tracker. Shown is a quarter section of the tracker. 2S modules are indicated as red lines ($r > 600 \text{ mm}$), PS modules as blue lines ($r > 600 \text{ mm}$). At lower radius and closer to the beam pipe is the pixel detector or Inner Tracker, which is not covered in this article. [5]

*Corresponding author

Email address: alexander.dierlamm@kit.edu (Alexander Dierlamm on behalf of the CMS Tracker Collaboration)

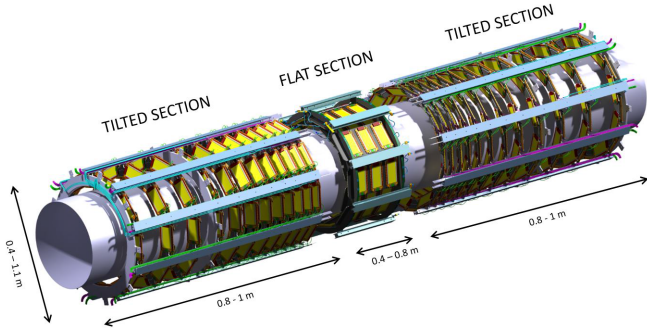


Figure 2: Drawing of the innermost layer of the barrel section, showing the central flat section and the two (identical) tilted sections. This layer also integrates the central part of the Inner Tracker support tube, as visible inside. [5]

two silicon sensors with a gap of 1.6 to 4.0 mm. These modules are specially designed to provide hits for each bunch crossing.

The 13296 modules are arranged in barrel layers in the center and as double discs in the endcap regions. The inner barrel has a novel tilted geometry for better tracking and reduced number of modules (i.e. lower material budget and costs), which is illustrated in Fig. 2. The temperature of the modules is controlled via two-phase CO₂ cooling (around -33 °C) being distributed with thin pipes also reducing the material budget. The electronic components on the modules are powered via DC-DC converters, which convert 11 V input voltage to the desired lower voltages. This reduces the required cable mass considerably.

All these implementations lead to a new tracker with reduced material in the tracking region and better performance at high pile-up than the current tracker at CMS.

3. p_T-module concept, Track Finder and L1-trigger

The design of the modules is driven by the need of hit information for each bunch crossing. It is not possible to transfer all hit information to the back-end readout system and therefore, the module needs to select relevant hits thus reducing the amount of data being transmitted for each bunch crossing (while keeping all hit data in the readout chip buffers for a final trigger decision up to 12.5 μs later). This selection is performed by applying a cut on the transverse momentum of charged particles, which can be exploited in the high magnetic field of CMS. A programmable search window allows to select straight, i.e. high momentum, particles as illustrated in Fig. 3. A cut corresponding to 2 GeV/c already removes 99% of the particle tracks. The accepted short track segments including the position and bend information, referred to as stubs, are transferred to the back-end via high-speed optical links and further to the Data, Trigger and Control (DTC) system and Track Finder. In this path the data is processed and fitted track parameters are provided to the L1-trigger system within 4 μs. This massive computation task will

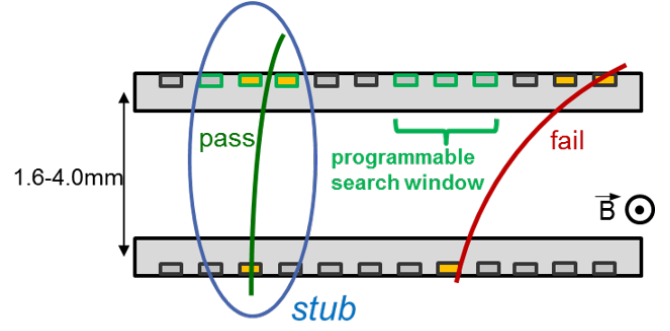


Figure 3: Illustration of the identification of particles with high transverse momentum. A hit in the lower sensor opens a programmable search window in the upper sensor such that particles with a momentum larger than about 2-3 GeV/c should pass through this sensor area. Such events are selected as trigger relevant data and shipped out as stubs.

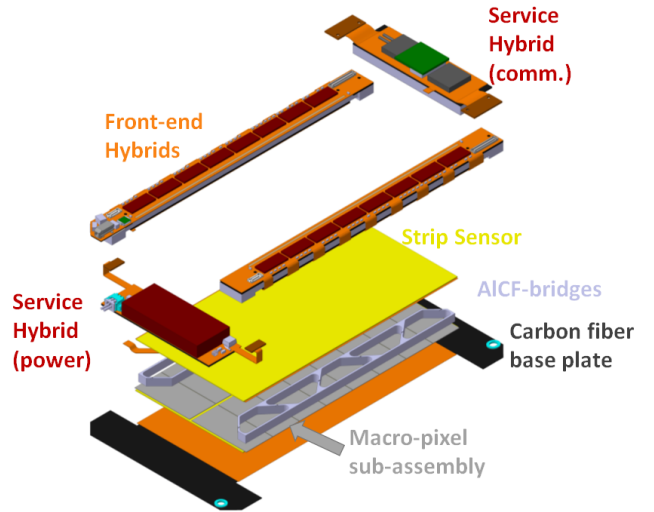


Figure 4: Drawing of the PS module type. Shown is the exploded view of parts as they need to be assembled at the module assembly sites. Adapted from [5].

be highly parallelized (time-multiplexing) and performed on many Track Finding Processors based on FPGAs as a reference system [5].

4. Module types and assembly

The inner modules of the Outer Tracker consist of strip sensors (2x960 strips with pitch of 100 μm and length of 2.5 cm) and pixel sensors (32x960 macro-pixel with pitch of 100 μm and length of 1.5 mm) and are called PS modules. This module type is illustrated in Fig. 4. The strip sensors of the PS module are connected to the strip sensor ASIC (SSA) [6], which sends hit information to the macro-pixel ASIC (MPA) [7], where the required correlation of hits in the upper strip sensor and the lower macro-pixel sensor is performed. These modules provide higher granularity due to the short macro-pixels, which is required for

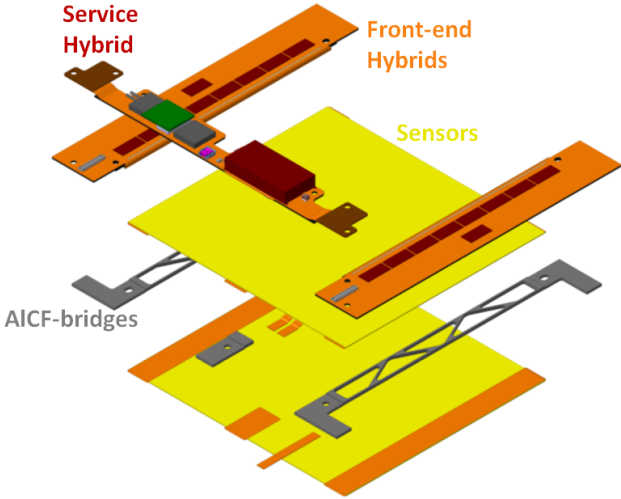


Figure 5: Drawing of the 2S module type. Shown is the exploded view of parts as they need to be assembled at the module assembly sites.

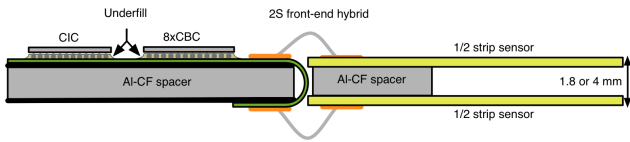


Figure 6: Illustration of the electrical connectivity of the front-end hybrid to the sensors on the 2S module. [5]

a good vertex resolution along the beam direction for L1-tracks. The expected maximum fluence for PS modules is $9.6 \times 10^{14} \text{ n}_{\text{eq}}/\text{cm}^2$ after 3000 fb^{-1} .

The **2S** modules consist of **2** strip sensors (2×1024 strips with pitch of $90 \mu\text{m}$ and length of 5 cm) (Fig. 5). The readout chips (CMS Binary Chip, CBC) [8] are connected to the upper and lower sensors via metal routing lines on the flex hybrid.

Both module types contain all necessary readout (readout chips as well as aggregation and formatting stage) and service (power and communication) components and are operated as standalone readout entities. The expected maximum fluence for 2S modules is $3 \times 10^{14} \text{ n}_{\text{eq}}/\text{cm}^2$ after 3000 fb^{-1} .

A crucial aspect for both module types is the connection of the individual readout chips to both sensor layers. This is realized by flex Kapton hybrids bent around a stiffener providing bond pads on both sides and traces to connect to the bump bonded readout chips. This is illustrated in Fig. 6 for the 2S module, but the concept applies to both module types.

The assembly of such modules demands very high precision on the parallelism of the upper and lower sensor strips or pixel columns. An angle between the sensors would cause the programmed search window to move depending on the hit location along the strip. This in turn affects

the p_T -resolution and deteriorates the efficiency of the p_T -discrimination for L1-tracks. The requirement on the angle between the upper and lower strips is set to $400 \mu\text{rad}$ for 2S modules ($800 \mu\text{rad}$ for PS), and motivated by the fact that the strips should not deviate more than $\pm 20 \mu\text{m}$ (less than half the pitch) along their length. Parallel offsets can be accounted for by configuring the chips accordingly and are not affecting the stub finding. The necessary accuracy is achieved by exploiting the good dicing precision (standard quality without requesting high accuracy) of the sensor manufacturers and assembly jigs with precision alignment pins. Methods to monitor the rotation between the upper and lower strips have been developed [5].

Modeling of the thermal performance of these modules was used to optimize the mass of the spacers, which are made of carbon fiber reinforced aluminum (AlCF, [9]) for very good thermal conductivity and a coefficient of thermal expansion (CTE) well matched to silicon. This can be achieved by controlling the volume of carbon fibers leading to a combined CTE. The cooling strategy for the two module types is slightly different. While the 2S modules are fixed on five points to the cooling pipe via small cooling blocks, the PS module is cooled via the whole back-surface of the macro-pixel sensor. This surface cooling is realized by gluing the bare module (macro-pixel sub-assembly and strip sensor glued to the AlCF spacers) to a heat spreading carbon-fiber baseplate, which in turn is glued to a large area cooling joint (Sec. 5.3).

5. Examples from prototyping

This section shows examples of the ongoing developments and prototypes for the above introduced upgrade.

5.1. Sensors

Sensors with n-type electrodes in p-type silicon bulk were chosen as the baseline technology [10]. It was shown that proper strip isolation can be achieved by both p-stop and p-spray technologies. Irradiation studies with samples of different p-stop concentrations recommend a moderate implantation dose to reduce high field induced noise or break down effects [11].

Full-size 2S sensors have been produced with the baseline layout and characterized to meet the specifications. Strip sensors with active thicknesses of $200 \mu\text{m}$, $240 \mu\text{m}$ and $300 \mu\text{m}$ were tested for their radiation hardness. The aims were a high signal over threshold and a stable annealing behavior. The latter was found for strip sensors with a thickness of $240 \mu\text{m}$ and below as shown in Fig. 7. The most probable value (MPV) of the signal distribution should be three times above the threshold to be highly efficient and the threshold should be set to about four times the noise to reduce the fraction of falsely identified hits to less than 10^{-4} . This results in a factor of twelve higher MPV of the seed signal (seed signal is more relevant than cluster signal due to the applied threshold cut)

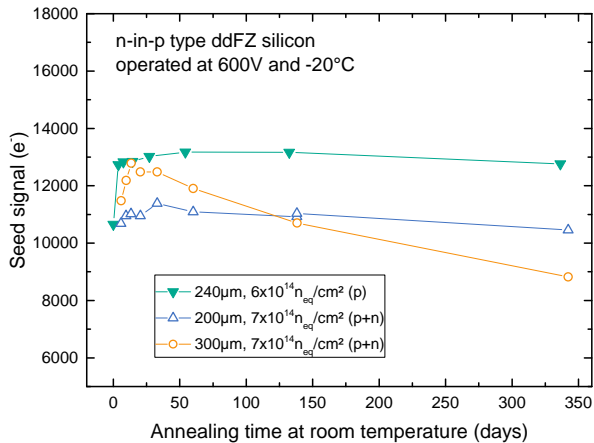


Figure 7: Annealing of the seed signal for irradiated thick (300 μm) and thin (200 μm and 240 μm) sensors. The annealing was performed at 60 $^{\circ}\text{C}$ and the duration scaled to room temperature via the scaling factor of leakage current according to [12]. [5]

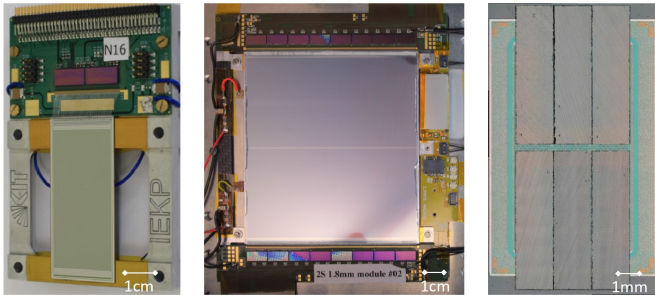


Figure 8: Images of prototype modules. From left to right: 2S mini module, full-size 2S module with prototype service hybrid, small macro-pixel sub-assembly with six chips. [5]

compared to the the noise figure of the readout chip with attached sensor. Sensors for 2S modules are required to provide a signal of 12 000 electrons due to a noise of about 1000 electrons, while strip sensors of the PS module (SSA chip with about 700 electrons noise connected to a 2.5 cm long strip) should exceed 8400 electrons. For macro-pixel sensors 4000 electrons are sufficient. Therefore, the current baseline is 240 μm for strip sensors and 200 μm for macro-pixel.

5.2. Modules

A first prototype module for the demonstration of stub finding was assembled from two small sensor prototypes and a rigid front-end hybrid containing two CBC chips of version 2. The sensors have 256 5 cm long strips at 90 μm pitch and are spaced by about 3 mm. Such modules (Fig. 8 left) are rotated in a particle beam (at CERN SPS and DESY) to emulate the bending of the particles in the detector's magnetic field. Fig. 9 demonstrated that the stub finding works efficiently before and after irradiating the modules to about double the expected fluence. Finally, full-size 2S modules (fig. 8 center) were assembled

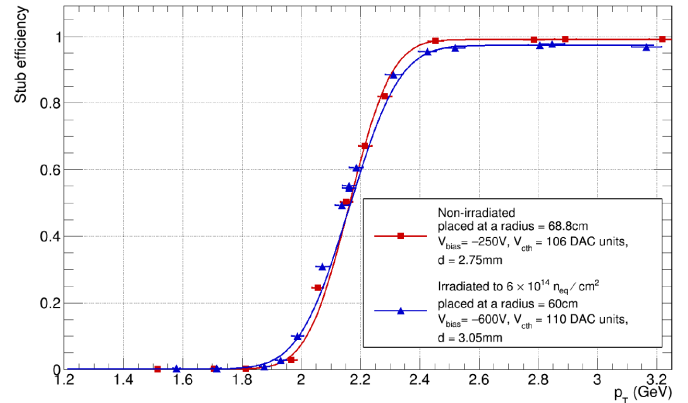


Figure 9: Stub reconstruction efficiency for a non-irradiated (red) and an irradiated (blue) 2S mini-module. The mini-module was irradiated to a fluence of 6×10^{14} $n_{\text{eq}}/\text{cm}^2$. The variable V_{cth} refers to the threshold setting, while d is the sensor spacing. Slightly different radii around 65 cm were used to calculate the momentum compensating for the fact that the modules had different sensor spacing but were operated with the same stub acceptance window. [5]

and characterized in particle beams (at CERN and FNAL) confirming good uniformity of the hit detection efficiency over the module width.

Such a large module was also used to study the influence of the DC-DC powering with a prototype service hybrid containing shielded air coils as inductors. Fig. 10 shows that the noise of the closest CBC increased slightly compared to direct powering but stayed below the specified 1000 electrons.

Also a small version of the macro-pixel sub-assembly (six small macro pixel ASICs bump bonded to a miniature macro-pixel sensor; Fig. 8 right) was designed and several assemblies produced. They were successfully operated at test beams and show, as indicated in Fig. 11, very high efficiency in a wide window of the clock phase.

5.3. Mechanics

The new mechanical challenge is the tilted geometry for the inner layers housing PS modules and to provide the large area cooling joints for this module type. The inner layers are grouped in ring structures, which provide cold surfaces on which the modules can be glued (Fig. 12). In the endcaps the cooling joints are embedded in the carbon-fiber sheets. A small prototype section was produced to learn about the manufacturing process and to study the transition region between the inner region populated with PS modules and the outer region populated with 2S modules. An image showing the measured temperature distribution with this prototype is presented in Fig. 13.

5.4. Track Finder

The feasibility of track finding within the given time window of 4 μs , transverse momentum resolution of about 2%, longitudinal vertex position resolution of about 1 mm

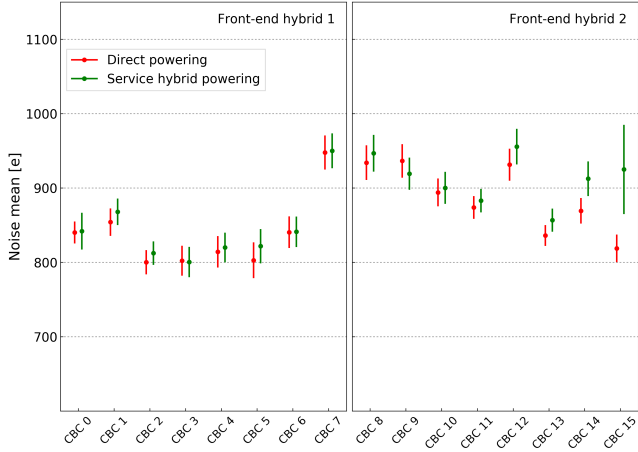


Figure 10: Average noise values for the 16 CBCs on both hybrids of a 2S module. The power was either provided directly from the lab power supply (red) or via the DC-DC converter on a prototype service hybrid (green). CBC15 is closest to the shielded air coils of the DC-DC converter (upper right CBC in Fig. 8 center). [5]

and a significant rate reduction of 1/100 was demonstrated in hardware by three approaches [5]. All of them need to go through four stages: data organization, pattern recognition, track fitting and duplicate removal. The data is grouped in regions and the hardware multiplied for time-multiplexing. One approach also uses associative memory chips for the pattern recognition [13], the other two are pure FPGA based [14, 15]. The latter have been chosen to be further developed on common hardware to optimize the FPGA-only reference system [5].

6. Conclusion and Outlook

All the new concepts of the upgraded CMS Tracker have been validated and the corresponding Technical Design Report was approved by December 2017 [5]. The community will increase the quantity of prototypes to finalize the assembly processes and to allow more intensive system and integration tests. The quality assurance for all parts is being reviewed and quality control mechanisms will be detailed.

The prototyping phase will continue with focus on large-scale production until pre-series productions are launched around 2020/21. The installation and commissioning of the final detector is foreseen for 2025.

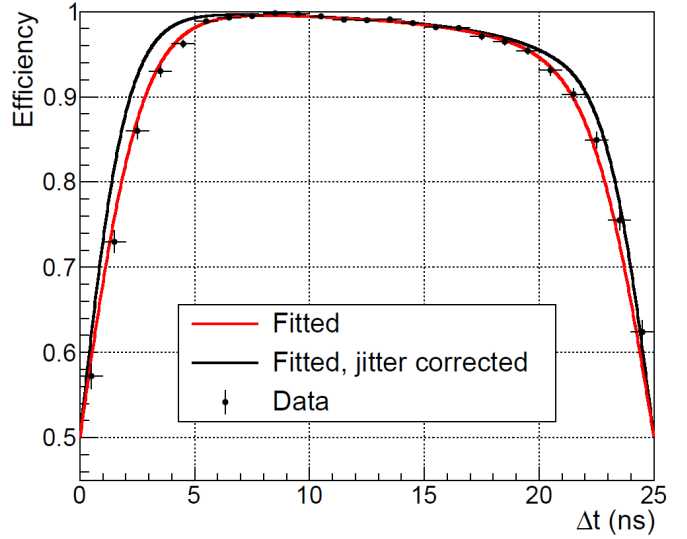


Figure 11: Efficiency of the hit identification with a small macro-pixel sub-assembly prototype. The efficiency is plotted versus the trigger arrival phase. The timing jitter in the system was determined and the profile was deconvoluted accordingly. [5]

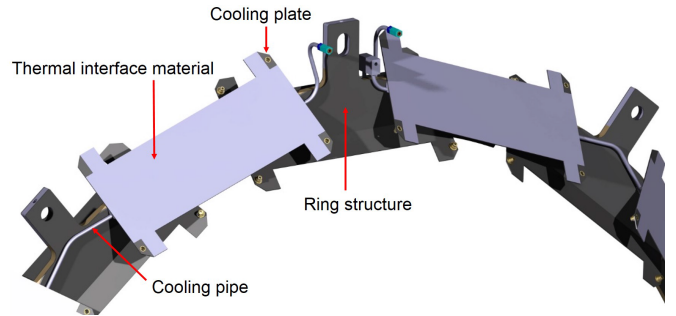


Figure 12: CAD study of the tilted ring geometry including cooling pipe routing and cooling plates. [5]

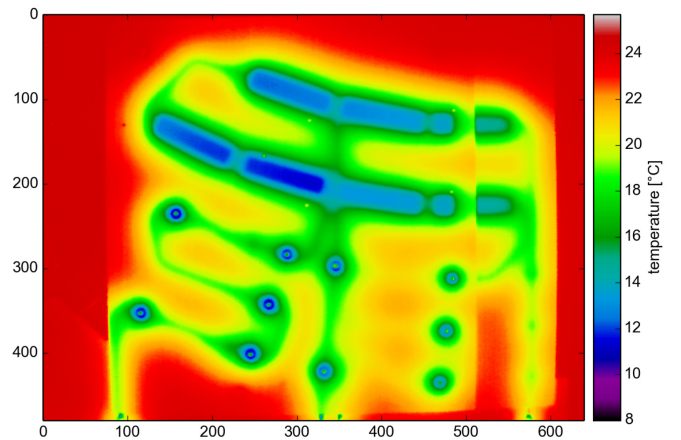


Figure 13: Thermographic image of a small prototype section of an endcap disk, when cooled with CO₂. The section was selected to study the transition region between the inner PS positions (larger blue bands) and the outer 2S positions (five point geometry). [5]

References

- [1] <http://hilumilhc.web.cern.ch/about/hl-lhc-project>.
- [2] I. Bejar Alonso, L. Rossi, HiLumi LHC Technical Design Report, CERN-ACC-2015-0140 (2015). <https://cds.cern.ch/record/2069130>.
- [3] CMS Collaboration, The CMS experiment at the CERN LHC, JINST 3 S08004 (2008).
- [4] CMS Collaboration, Technical Proposal for the Phase-II Upgrade of the CMS Detector, CERN-LHCC-2015-010 (2015). <https://cds.cern.ch/record/2020886>
- [5] CMS Collaboration, The Phase-2 Upgrade of the CMS Tracker, CERN-LHCC-2017-009 (2017). <https://cds.cern.ch/record/2272264>.
- [6] K. Kloukinas et al., Short-Strip ASIC (SSA): A 65nm Silicon-Strip Readout ASIC for the Pixel-Strip (PS) Module of the CMS Outer Tracker Detector Upgrade at HL-LHC, PoS(TWEPP-17)031.
- [7] D. Ceresa et al., A 65 nm pixel readout ASIC with quick transverse momentum discrimination capabilities for the CMS Tracker at HL-LHC, JINST 11 (2016) C01054.
- [8] D. Braga et al., CBC2: A microstrip readout ASIC with coincidence logic for trigger primitives at HL-LHC, JINST 7 (2012) C10003.
- [9] S. Seshan, A. Guruprasad, M. Prabha and A. Sudhakar, Fibre-reinforced metal matrix composites – a review, J. Indian Inst. Sci. 76, 1-14 (1996). <http://journal.library.iisc.ernet.in/index.php/iisc/article/viewFile/2575/4137>.
- [10] A. Dierlamm et al., P-Type Silicon Strip Sensors for the new CMS Tracker at HL-LHC, JINST 12 (2017) P06018.
- [11] M. Printz, P-stop isolation study of irradiated n-in-p type silicon strip sensors for harsh radiation environments, NIM A 831 (2016) 3843.
- [12] M. Moll, Radiation Damage in Silicon Particle Detectors, University of Hamburg, PhD thesis, DESY-THESIS-1999-040 (1999).
- [13] A. Rossi et al., A Track Finder with Associative Memories and FPGAs for the L1 Trigger of the CMS experiment at HL-LHC, this issue.
- [14] I. Tomalin et al., An FPGA based track finder for the L1 trigger of the CMS experiment at the High Luminosity LHC, JINST 12 (2017) P12019 .
- [15] M. Zientek et al., FPGA-Based Tracklet Approach to Level-1 Track Finding at CMS for the HL-LHC, EPJ Web of Conferences 150, 00016 (2017).